



UNIVERSITY OF LEEDS

This is a repository copy of *In vivo biocompatibility of custom-fabricated apatite-wollastonite-mesenchymal stromal cell constructs.*

White Rose Research Online URL for this paper:  
<http://eprints.whiterose.ac.uk/84530/>

Version: Accepted Version

---

**Article:**

Lee, JA, Knight, CA, Kun, X et al. (4 more authors) (2015) In vivo biocompatibility of custom-fabricated apatite-wollastonite-mesenchymal stromal cell constructs. *Journal of biomedical materials research. Part A*. ISSN 1549-3296

<https://doi.org/10.1002/jbm.a.35448>

---

**Reuse**

Unless indicated otherwise, fulltext items are protected by copyright with all rights reserved. The copyright exception in section 29 of the Copyright, Designs and Patents Act 1988 allows the making of a single copy solely for the purpose of non-commercial research or private study within the limits of fair dealing. The publisher or other rights-holder may allow further reproduction and re-use of this version - refer to the White Rose Research Online record for this item. Where records identify the publisher as the copyright holder, users can verify any specific terms of use on the publisher's website.

**Takedown**

If you consider content in White Rose Research Online to be in breach of UK law, please notify us by emailing [eprints@whiterose.ac.uk](mailto:eprints@whiterose.ac.uk) including the URL of the record and the reason for the withdrawal request.



[eprints@whiterose.ac.uk](mailto:eprints@whiterose.ac.uk)  
<https://eprints.whiterose.ac.uk/>

***In vivo* biocompatibility of custom-fabricated apatite-wollastonite-mesenchymal stromal cell constructs<sup>3</sup>**

**Jennifer A Lee<sup>1,2</sup>, Charlotte A Knight<sup>1</sup>, Xiao Kun<sup>2</sup>, Xuebin B Yang<sup>2</sup>, David J Wood<sup>2</sup>, Kenneth W Dalgarno<sup>3</sup> and Paul G Genever<sup>1</sup>**

<sup>1</sup>Department of Biology, University of York, York, YO10 5YW, United Kingdom.

<sup>2</sup>Biomaterials and Tissue Engineering Research Group, School of Dentistry, University of Leeds, Leeds, LS2 9LU, United Kingdom. <sup>3</sup>School of Mechanical and Systems Engineering, Newcastle University, Newcastle, NE1 7RU, United Kingdom

E-mail: [paul.genever@york.ac.uk](mailto:paul.genever@york.ac.uk)

**Short Title:**

Custom AW-cell constructs *in vivo*

This article has been accepted for publication and undergone full peer review but has not been through the copyediting, typesetting, pagination and proofreading process which may lead to differences between this version and the Version of Record. Please cite this article as an 'Accepted Article', doi: 10.1002/jbm.a.35448

## Abstract

We have used the additive manufacturing technology of selective laser sintering (SLS), together with post SLS heat treatment, to produce porous three dimensional scaffolds from the glass-ceramic apatite-wollastonite (A-W). The A-W scaffolds were custom-designed to incorporate a cylindrical central channel to increase cell penetration and medium flow to the centre of the scaffolds under dynamic culture conditions during *in vitro* testing and subsequent *in vivo* implantation. The scaffolds were seeded with human bone marrow mesenchymal stromal cells (MSCs) and cultured in spinner flasks. Using confocal and scanning electron microscopy, we demonstrated that MSCs formed and maintained a confluent layer of viable cells on all surfaces of the A-W scaffolds during dynamic culture. MSC-seeded, with and without osteogenic pre-differentiation, and unseeded A-W scaffolds were implanted subcutaneously in MF1 nude mice where osteoid formation and tissue in-growth were observed following histological assessment. The results demonstrate that the *in vivo* biocompatibility and osteo-supportive capacity of A-W scaffolds can be enhanced by SLS-custom design, without the requirement for osteogenic pre-induction, to advance their potential as patient-specific bone replacement materials.

## Keywords

Apatite-wollastonite, glass-ceramic, selective laser sintering, mesenchymal stromal cells, *in vivo* biocompatibility.

## Introduction

The production of anatomically correct surgical models has paved the way for the development of bone grafts designed to patient specific geometries [1, 2]. Solid freeform fabrication (SFF) is one of the enabling technology platforms that is allowing the production of three dimensional (3D) scaffolds with complex geometries containing internal

architectures for tissue regeneration [3-5]. Scaffolds can be custom-designed for individual patients using, for example, data collated from computed tomography (CT) scans, allowing for the inclusion of precise structural properties and levels of porosity to mimic the desired tissue type [3]. Selective laser sintering (SLS) is one of these SFF technologies and works through use of a laser to consolidate layers of powdered raw material into a 3D structure [6]. Simpson et al used SLS in combination with CT scan data to produce a model human phalanx from a poly(L-lactide-co-glycolide)/ $\beta$ -tricalcium-phosphate composite [7] and Mangano and co-workers used a custom made SLS titanium blade for treatment of patients with severely atrophied posterior mandibles [8]. In addition, fused deposition modelling, another SFF technology has been successfully used to produce customized PCL scaffolds to repair critical sized complex cranial defects in rabbits [9]. Patient-specific grafts have now been applied clinically, for example Warnke et al successfully repaired an extended mandibular discontinuity defect in a human patient using CT data and computer aided design technology to create a Teflon model for a titanium mesh cage [10]. This was subsequently filled with bone mineral blocks infiltrated with both recombinant human BMP-7 and autologous bone marrow prior to transplantation into the mandibular defect; data obtained post-transplantation showed significant bone formation throughout the length of the mandible replacement [11].

Materials attractive for bone tissue engineering, such as glass-ceramics can also be applied to SLS technologies and we have previously used this method to produce bioactive 3D porous scaffolds from apatite-wollastonite (A-W) glass-ceramic [12, 13]. Coupled with excellent biocompatibility and resorption *in vivo*, A-W has a high mechanical strength due to the fact that the apatite phase lies within a fibrous wollastonite phase that helps block crack propagation [14-17]. A-W lends itself particularly well to SLS techniques allowing more complex components to be fabricated. The use of such a bioactive material is particularly appealing as it forms a direct physical bond to bone via the formation of an apatite layer on

the surface of the material helping to improve integration of the graft [14-16, 18, 19]. In addition, bone grafts are often seeded with osteoprogenitor cells to accelerate tissue regeneration and further integration. Mesenchymal stromal cells (MSCs) can be isolated from various adult and foetal tissues and demonstrate tri-lineage potency into osteogenic, chondrogenic and adipogenic lineages [20, 21]. Biomaterial scaffolds seeded with MSCs and implanted into bone defects are shown to exhibit increased integration compared to un-seeded controls [22]; as such MSCs are a prime candidate cell type for orthopaedic tissue engineering applications.

We have previously demonstrated that SLS 3D microporous A-W scaffolds with a basic design (bA-W scaffolds) support the attachment, proliferation and osteogenic differentiation of human MSCs *in vitro* [12]. However, microporosity at the levels obtained (typically less than 50  $\mu\text{m}$ ) does not allow for vascularisation. In the work presented in this paper we have used the flexibility of the manufacturing process to produce a model macro- and micro-porous structure and assessed its ability to promote vascularisation, with and without optimised seeding using osteogenic pre-differentiated and undifferentiated MSCs, in a subcutaneous mouse model. The customised A-W design (cA-W scaffolds) contains a 1mm diameter central channel, and to promote cell attachment a dynamic culture method has been used, with the intention of enhancing the integration and restoration of tissue *in vivo*.

### **Materials and methods**

All plasticware were purchased from Corning and all reagents were obtained from Invitrogen unless otherwise stated.

#### *Apatite-wollastonite scaffold production*

A-W glass-ceramic scaffolds were produced as previously described [13]. Briefly, a glass of molar composition  $7.1\text{MgO}\cdot 35.5\text{SiO}_2\cdot 7.1\text{P}_2\text{O}_5\cdot 49.9\text{CaO}\cdot 0.4\text{CaF}_2$ , was produced by mixing

the components (BDH Laboratory Supplies) shown in Table 1, followed by heating at 1450°C (I Temp 15/16, Pyrotherm), followed by shock quenching in water. 3D structures were produced by indirect SLS [13].

bA-W scaffolds were produced by mixing the 45-90 $\mu$ m powder fraction with an acrylic binder at 5% w/w composition (3D systems) using an experimental SLS machine, described in [23]. The laser sintering parameters were a laser power of 5W, scan speed of 150mm/s and an initial powder bed depth of 5mm. Consecutive scan lines were overlapped by 0.55mm with a spread layer depth of 0.125mm. The 'green body' scaffolds were sintered and crystallised by heating in a furnace to 779°C for 1 hour with an incremental heat increase of 10°C per minute before increasing to 1150°C for another hour (Lenton Thermal Designs), after which samples were cooled to room temperature, to produce bars with final dimensions of 25x3x2 mm. Subsequent characterisation revealed these had a microporosity of 35-37% (assessed by calculating an apparent density from measured dimensions and weight, and comparing this to the true density of A-W), flexural strength of 37 $\pm$ 5MPa [13] and pore sizes up to 50 $\mu$ m [24]. Using a precision cut off machine (Accutom 5, Struers) scaffolds were cut to dimension of 3x3x2mm. For the cA-W scaffold production, the 45-90 $\mu$ m and 0-45 $\mu$ m glass powder particle fractions were mixed in a 3:1 ratio and then combined with 10% w/w acrylic binder. Green parts with dimensions 5x5x2mm with a 1mm diameter cylindrical central channel were produced on a modified commercial SLS machine (Sinterstation 2000, 3D Systems), described in [24]. Scaffolds were made using a laser power of 25W, scan speed of 100mm/s and a powder bed depth of 10mm. Successive scan lines were overlapped by 0.2mm with a spread layer depth of 0.12mm. cA-W scaffolds were post processed using an identical heat treatment program as that used for the bA-W scaffolds. The nature of the crystal phases produced post heat-treatment were identified through X-ray diffraction using a Philips Analytical PW3050 X-ray diffractometer at 40keV, wavelength 1.5406 and a scan

range from 10-70° 2 $\theta$ . The smaller glass particle sizes in cA-W scaffolds reduced the overall microporosity level to 25-27% (with pore sizes up to 50 $\mu$ m), whilst the flexural strength increased to 69 $\pm$ 10MPa [24]. Both the bA-W and the cA-W scaffolds were sterilized by autoclaving at 15psi for 20 minutes at a temperature of 121°C.

#### *Isolation and culture of human MSCs*

Bone samples were obtained from Harrogate District Hospital, Harrogate, UK under approval by the Harrogate Local Research Ethics Committee. MSCs were extracted from the bone marrow of human femoral heads obtained with informed consent from routine hip replacement surgery as previously described [25]. To encourage osteogenic differentiation, cells were grown to confluence upon which the medium was replaced with basal medium containing osteogenic supplements (50 $\mu$ g/ml L-ascorbic acid phosphate, 5mM  $\beta$ -glycerophosphate and 10nM dexamethasone [Sigma-Aldrich]).

#### *Cell seeding and dynamic culture of A-W scaffolds*

Dynamic culture was carried out using 125ml spinner flasks (Techne), mechanized with a magnetic stirring platform (StemStirrer). Spinner flasks were coated with a silicone solution (Sigmacote, Sigma-Aldrich) to prevent cell attachment to the vessel surface, then sterilized by autoclaving. Scaffolds were immersed in basal medium at 37°C for 30 minutes to equilibrate, then placed into a non-adherent 96 U-bottomed well plate and the cells were pipetted in a volume of 100 $\mu$ l basal medium (1X DMEM, 10% FBS and 1% P/S) onto each scaffold. The cells were cultured for one hour before each scaffold was inverted, placed in a fresh well and the remaining MSCs from the first wells were re-applied to the scaffolds and left for a further hour. Each scaffold was transferred to basal medium, prior to spinner flask culture in 30ml basal medium with continual stirring at 30rpm. After 24 hours spinner flask culture the basal medium was replaced with osteogenic medium and the media changed every

3-4 days, unless otherwise stated. Cells were seeded on scaffolds in triplicate for each experimental time point.

#### *Seeding density optimisation and analysis.*

cA-W scaffolds were seeded with  $1 \times 10^6$ ,  $1.5 \times 10^6$  or  $2 \times 10^6$  MSCs per scaffold and proportionally the same number for the bA-W scaffolds at  $5 \times 10^5$  or  $1 \times 10^6$  MSCs per scaffold.

Seeded scaffolds were analysed by scanning electron microscopy (SEM, Jeol JSM-6490LV) after 24 hours spinner flask culture in basal medium. Scaffolds were fixed overnight with 2.5% glutaraldehyde in phosphate buffer (77mM  $\text{Na}_2\text{HPO}_4$ , 23mM  $\text{NaH}_2\text{PO}_4$ ); then dehydrated with a graded series of ethanols (30%, 50%, 70%, 90%) for 30 minutes each, followed by three changes of 100% ethanol for 30 minutes each. Subsequently, scaffolds were immersed in hexamethyldisilazane (HMDS, Sigma-Aldrich) and left to dry overnight in a sealed desiccated container. Scaffolds were placed in an argon atmosphere then either sputter coated with gold for 30 seconds at 40mA (Agar) or sputter coated with gold at 2kV for 1 minute (Polaron), after which they were analysed by SEM (Jeol JSM-6490LV).

#### *Cell viability determination*

Cell viability was determined using a live/dead assay (Invitrogen), consisting of calcein AM and ethidium homodimer-1 fluorescent stains and carried out following the manufacturer's instructions. Cells were visualized using a Zeiss LSM 510 meta on an Axiovert 200M confocal microscope. All confocal images are condensed z-stack images.

#### *Subcutaneous implantation of A-W scaffolds in nude mice*

All *in vivo* experiments were carried out in accordance with ethical guidelines under the Home Office project licence of Dr Xuebin Yang, University of Leeds, UK. NIH guidelines for the care and use of laboratory animals (NIH Publication #85-23 Rev. 1985) have been

observed. cA-W and bA-W scaffolds were seeded with  $2 \times 10^6$  and  $1 \times 10^6$  MSCs per scaffold respectively and transferred to spinner flasks for 24 hours culture in basal medium. Scaffold-MSCs constructs were either implanted directly or dynamically cultured for a further 6 days in osteogenic medium before implantation (Table 2). Control un-seeded cA-W scaffolds were also implanted. Four replicates were included for each treatment group. Seven week old male MF1 athymic nude mice were anesthetized by intraperitoneal injection with a 1:1 mixture of Hypnorm (1:4 in sterile H<sub>2</sub>O; Leeds, UK)/Hypnovel (1:1 in sterile H<sub>2</sub>O, Midazolam, Roche) (8ml/kg) [26]. A 1 cm incision was made on each side of the back and a subcutaneous pocket created by blunt dissection. A single scaffold was inserted into each subcutaneous pocket, after which the incision was closed with non-resorbable sutures (5-0 Ethilon, Ethicon). Mice were sacrificed after 4 or 8 weeks and the scaffolds analysed by histological staining. Scaffolds and surrounding tissue were extracted after 4 weeks and examined for evidence of inflammation or vascularisation.

#### *Resin embedding and sectioning*

Following removal from the implant site, scaffolds were fixed in 10% neutral buffered formaldehyde for 24 hours, followed by ethanol dehydration (30%, 50%, 70%, 90% and 3 x 100%) for 30 minutes each. Scaffolds were placed in a 1:1 mixture of 100% ethanol and methacrylate resin (Sigma-Aldrich) and agitated for 72 hours, followed by agitation in 100% methacrylate resin for a further 48 hours. Scaffolds were then placed in methacrylate resin containing 1% w/v benzoyl peroxide (Sigma-Aldrich) and incubated at 50°C overnight to allow the resin to polymerize. 300µm sections were cut using a precision cut off machine (Accutom-5, Struers). The sections were then polished to a thickness of 100µm using P600 and P1200 Wet or dry Tri-M-ite (3M).

### *Sanderson's rapid bone stain*

Sections were stained with Sanderson's rapid bone stain (Surgipath) for 2 minutes at 55°C then washed with dH<sub>2</sub>O. Sections were then counter-stained with van Gieson (Raymond A. Lamb Ltd) for 5 minutes, cleared in xylene for 5 minutes and mounted on glass microscope slides with DPX (BDH). Sections were analysed by standard light microscopy (DMLA, Leica).

### *Alcian blue/sirius red staining*

Sections were stained with Weigart's haematoxylin (equal parts of 1g haematoxylin [Surgipath] in 100ml absolute ethanol; and 30% aqueous ferric chloride [BDH], 1ml concentrated HCl in 95ml dH<sub>2</sub>O), then submerged briefly in 1% HCl in absolute methanol. After which scaffolds were stained with alcian blue (0.5g alcian blue 8GX [Sigma-Aldrich] with 1ml acetic acid in 100ml dH<sub>2</sub>O) for 10 minutes and treated with 1% phosphomolybdic acid for 20 minutes, before staining with sirius red (0.3% sirius red [BDH] in saturated picric acid) for 60 minutes. Sections were dehydrated with 100% ethanol, cleaned in xylene for 5 minutes and mounted on glass microscope slides with DPX. Sections were analysed with standard light microscopy (DMLA, Leica).

## **Results**

### *Scaffold design and seeding density optimisation*

A-W scaffolds were produced with a basic design (bA-W) and a custom-designed 1mm cylindrical central channel (cA-W) (Fig. 1). Fig. 2 shows an exemplary XRD pattern of the sintered material, demonstrating that the temperature cycle used produced the desired fluorapatite (ICDD 15-876) and wollastonite (ICDD 42-547) phases, with a significant residual glassy phase also present. The weight ratio of these phases has been reported to be in the range ~32-35:25-40:25-40 depending upon precise heat treatment [15, 27]. Few surface

details of either apatite or wollastonite crystals are visible via SEM; high magnification images revealed small domains of interlocked crystals similar to those observed by Kokubo et al [27, 28]. Seeding density analysis on cA-W scaffolds was used to optimise initial cell seeding numbers; we have previously determined static seeding efficiency on bA-W scaffolds [12]; we found that different initial seeding densities were required for bA-W and cA-W to generate a confluent monolayer across the scaffolds, avoiding cell stacking and ensuring efficient use of the primary cells. This was primarily due to the size and surface area difference between bA-W and cA-W scaffolds, and was calculated over three separate experiments. MSCs were statically seeded on cA-W scaffolds at densities of  $1 \times 10^6$ ,  $1.5 \times 10^6$  and  $2 \times 10^6$  cells per scaffold, dynamically cultured in spinner flasks at 30rpm for 24 hours and analysed by SEM (Fig. 3A-C). The results identified that  $2 \times 10^6$  cells per scaffold was the optimal seeding density. This number gave a confluent layer of cells across the whole surface of the scaffold, which would be conducive for osteogenic differentiation. At seeding densities of  $1 \times 10^6$  or  $1.5 \times 10^6$  cells per scaffold bare patches of scaffold in-between confluent areas of cells could be observed. A similar process was performed for bA-W scaffolds (Fig. 3D-E) and determined that  $1 \times 10^6$  cells per scaffold was optimal. The optimal seeding density for bA-W scaffolds was also determined by seeding the scaffolds with  $5 \times 10^5$  or  $1 \times 10^6$  MSCs per scaffold, followed by dynamic culture for 24 hours and analysis by SEM (Fig. 3D-E). Here,  $1 \times 10^6$  cells per scaffold were optimal for bA-W scaffolds.

#### *Viability and morphology of MSCs dynamically cultured on cA-W scaffolds*

MSCs were seeded on cA-W scaffolds at a density of  $2 \times 10^6$  cells per scaffold and 24 hours after spinner flask culture the medium was changed to osteogenic medium. Cell viability was determined using a fluorescent live/dead assay and confocal microscopy 0, 7, 14 and 21 days after osteogenic induction. The results demonstrated that MSCs remained viable (green fluorescence) for up to 21 days when cultured on the scaffolds with minimal compromised

cells (Fig. 4). Day 0 is the equivalent of Day 1 in basal media. Scaffolds were analysed by SEM at 0, 7, 14 and 21 days after osteogenic induction to determine MSC growth and spreading (Fig. 5). The MSCs produced a confluent sheet of elongated spindle-shaped cells on all outer surfaces of the scaffold including the central channel after 24 hours culture, and maintained confluency for the 3 week culture period. By 14 days culture the central channel was completely covered by cells and/or matrix. Results demonstrated that dynamic culture was conducive to MSCs adherence, spreading and viability for up to 21 days of dynamic culture. Similar results have been seen previously for bA-W scaffolds [12].

#### *Subcutaneous implantation of MSC seeded A-W scaffolds in vivo*

All MSC-seeded scaffolds, extracted 4 weeks after implantation, stained positively for osteoid and soft tissues in the pores and around the periphery of the scaffolds using Sanderson's rapid bone stain (Fig. 6). The scaffolds also demonstrated good integration with the host soft tissue. However, for both the cA-W and bA-W scaffolds there was no obvious difference in the amount of osteoid staining between MSC-seeded scaffolds cultured in basal or osteogenic medium. The differences in geometry and porosity of the cA-W and bA-W scaffolds seem to have made no significant difference to the amount of osteoid staining. There was a greater level of osteoid staining in the central channel and periphery of MSC-seeded cA-W scaffolds (Fig. 6, C1, C2 and D1, D2) compared to the un-seeded control (Fig. 6, E1, E2). There was an enhanced level of osteoid staining both in the pores and around the periphery of all the scaffolds after 8 weeks implantation (Fig. 7) compared to 4 weeks (Fig. 6). Cells can be observed attached to the surface of the scaffolds and in the surrounding pores. Again, for both the cA-W and bA-W scaffolds there was no obvious difference in the amount of staining between MSC-seeded scaffolds cultured in basal or osteogenic medium. There was more uniformity of osteoid staining in the central channel of MSC-seeded cA-W scaffolds (Fig. 7, C3 and D3) compared to the un-seeded control (Fig. 7, E3). However, the

amount of staining in the main body of the seeded and un-seeded cA-W scaffolds was similar. Results demonstrate that the scaffolds integrate well into the host tissue and support the formation of osteoid particularly in MSC-seeded samples. Importantly, an osteogenic pre-differentiation step did not enhance osteoid deposition.

Sectioned scaffolds were stained with alcian blue and sirius red for cartilage and collagen matrices respectively. After 4 weeks implantation, positive sirius red staining was observed on the surface and in the pores of all the scaffolds (Fig. 8). However, there was no positive alcian blue staining. For both the cA-W and bA-W scaffolds there was no obvious difference in the amount of staining between MSC-seeded scaffolds cultured in basal or osteogenic medium. There was an enhanced level of sirius red staining in the central channel of seeded cA-W scaffolds (Fig. 8, C3 and D3) compared to the un-seeded control (Fig. 8, E3). In the main body of the scaffolds there also appeared to be more intense red staining in the cA-W group (Fig. 8, C2-E2) compared to that in the bA-W group (Fig. 8, A2 and B2), indicating that more collagen matrix was deposited within the cA-W scaffolds. However, the amount of staining in the main body of the seeded and un-seeded cA-W scaffolds was similar (Fig. 8, C2-E2). There was no observable difference in the level of alcian blue/sirius red staining in the scaffolds after 8 weeks implantation compared to 4 weeks (data not shown). Further to this, macroscopic examination of cA-W scaffolds cultured *in vivo* for 4 weeks showed signs of blood vessels surrounding the scaffold constructs, particularly around/towards the central channel (Fig. 9). Results demonstrate that the scaffolds support collagen matrix formation *in vivo* and that cA-W scaffolds may be more conducive to collagen matrix deposition and blood vessel localisation due to their macro-porous design.

## Discussion

We aimed to produce an A-W bone replacement scaffold to a specific geometry that would support the dynamic culture and *in vivo* bone forming capacity of human MSCs. We have

demonstrated that A-W scaffolds produced by SLS to a specified shape and size could be seeded with a confluent layer of cells on all surfaces, and that they remained viable and attached to the scaffolds for 21 days of spinner flask culture. cA-W and bA-W scaffolds were seeded with MSCs then pre-cultured in either basal or osteogenic medium and implanted subcutaneously in nude mice. Good integration with the host tissue and osteoid formation was observed in both scaffolds, along with evidence of vascularisation, more so in cA-W compared to bA-W. The *in vivo* experiments were carried out in quadruplicate with representative images shown; the observations were reproducible but qualitative and warrant further quantitative analysis and statistical testing.

There was a high level of viability of MSCs after 24 hours of spinner flask culture on the cA-W scaffolds, as determined by confocal analysis of live/dead staining, which was retained over three weeks of culture. SEM analysis of the cA-W scaffolds demonstrated that the MSCs remained attached to the scaffolds as a confluent layer for 3 weeks culture and by 14 days of dynamic culture the central channel was completely covered by cells and/or matrix. Cell proliferation may have been enhanced by the dynamic culture, an effect which has previously been reported [29-31], or the cells may have secreted extracellular matrix into the central channel. In addition to this, dynamic spinner flask culture has been shown to enhance osteogenic and adipogenic differentiation potential, an effect most likely due to changes in cytoskeletal arrangement and gene expression patterns [32]. The confluent nature of the cells seeded onto the surface of the scaffold could potentially reduce the flow of nutrients and gases between the outer and inner parts of the scaffold and thus affect cell penetration; however this does not appear to be the case from our observations *in vivo* where tissue was formed throughout the inner and outer parts of the scaffold. The combined macro and micro-porous nature of the cA-W scaffolds supports the theory that macroporosity allows enhanced early in-growth and matrix deposition within the central channel whilst the

microporosity allows controlled resorption over time, as Fjita et al demonstrated with *in vivo* implantation of microporous A-W scaffolds [33].

*In vivo* tissue in-growth was observed in both the cA-W and bA-W scaffolds as determined by Sanderson's rapid bone stain and alcian blue/sirius red staining after subcutaneous implantation in nude mice, and resulted in substantial integration with the host tissue indicating the potential of enhanced osteointegration for clinical application. It is likely that the observed tissue in-growth originated from a combination of implanted cells and cells from the surrounding tissue, particularly as A-W is biomimetic and as such encourages cell infiltration and attachment. As expected, there was more tissue formation in the 8 week samples compared to the 4 week samples, there was also substantial tissue formation observed in the central channel of the MSC-seeded cA-W scaffolds, which was greater than that observed in the un-seeded controls. All samples supported the formation of osteoid, identified by bright green/blue Sanderson's rapid bone staining. There was no obvious difference in osteoid formation between un-seeded and seeded cA-W scaffolds by week 8, however at week 4 there appeared to be a higher level of osteoid deposition in the seeded scaffolds compared to the un-seeded scaffolds. These observations suggest that MSC-seeded scaffolds enhance initial matrix and osteoid formation to facilitate earlier repair than those scaffolds implanted without MSCs. Furthermore, seeded scaffolds showed increased tissue formation in the channel of cA-W scaffolds compared to un-seeded cA-W scaffolds, demonstrating that populating with MSCs could facilitate a higher rate of tissue formation in larger channels and pores. It is thought that pre-differentiating MSCs before *in vivo* implantation can enhance their osteogenic potential [34]. However, we found no difference in the tissue forming capacity of MSCs cultured on A-W scaffolds in basal medium for 1 day or osteogenic medium for 7 days. This observation aligns itself to other studies where pre-culture time of MSCs was varied before subcutaneous or cranial implantation into rats, results

of which demonstrated that increasing pre-culture time decreased *in vivo* bone formation [35, 36]. Macroscopic examination of cA-W scaffolds 4 weeks post implantation revealed blood vessel association surrounding the scaffold, particularly near the central channel. Blood vessel infiltration would help facilitate successful osteointegration of the construct when implanted orthotopically. The differences in fabrication route, geometry and porosity of the cA-W and bA-W scaffolds made no significant difference in the degree of osteoid formation within the main body or periphery of the scaffold structures. There was a high degree of collagen formation in all samples as determined by sirius red staining; however there was more intensive staining in the cA-W group compared to the bA-W group, indicating higher collagen matrix deposition within the cA-W scaffolds at four weeks. This may be due to the greater cell and nutrient infiltration into the centre of the cA-W scaffolds compared to the bA-W due to an increased surface area and accessibility within the centre channel, thus facilitating penetration of cells and subsequent tissue regeneration.

Therefore, optimally MSC pre-seeded custom-designed scaffolds, without osteogenic predifferentiation offers an appropriate route for bone replacement using A-W glass-ceramics.

### **Acknowledgements**

The authors thank the patients and staff at Harrogate District Hospital and Clifton Park Hospital, York for the supply of bone samples and Simon Palmer for help with the *in vivo* study. We would also like to thank the White Rose University Consortium and Arthritis Research UK Tissue Engineering Centre (19429) for funding this research.

## References

1. Li JH, Zhang L, Lv SY, Li SJ, Wang N, Zhang ZT 2011 Fabrication of individual scaffolds based on a patient-specific alveolar bone defect model *Journal of Biotechnology*. **151** 87-93
2. Grayson WL, Frohlich M, Yeager K, Bhumiratana S, Chan ME, Cannizzaro C, et al. 2010 Engineering anatomically shaped human bone grafts *Proc Natl Acad Sci U S A*. **107** 3299-304
3. Leong KF, Cheah CM, Chua CK 2003 Solid freeform fabrication of three-dimensional scaffolds for engineering replacement tissues and organs *Biomaterials*. **24** 2363-78
4. Seitz H, Rieder W, Irsen S, Leukers B, Tille C 2005 Three-dimensional printing of porous ceramic scaffolds for bone tissue engineering *Journal of Biomedical Materials Research Part B-Applied Biomaterials*. **74B** 782-8
5. Lee JS, Cha HD, Shim JH, Jung JW, Kim JY, Cho DW 2012 Effect of pore architecture and stacking direction on mechanical properties of solid freeform fabrication-based scaffold for bone tissue engineering *Journal of Biomedical Materials Research Part A*. **100A** 1846-53
6. Berry E, Brown JM, Connell M, Craven CM, Efford ND, Radjenovic A, et al. 1997 Preliminary experience with medical applications of rapid prototyping by selective laser sintering *Medical Engineering & Physics*. **19** 90-6
7. Simpson RL, Wiria FE, Amis AA, Chua CK, Leong KF, Hansen UN, et al. 2008 Development of a 95/5 poly(L-lactide-co-glycolide)/hydroxylapatite and beta-tricalcium phosphate scaffold as bone replacement material via selective laser sintering *Journal of Biomedical Materials Research Part B-Applied Biomaterials*. **84B** 17-25
8. Mangano F, Bazzoli M, Tettamanti L, Farronato D, Maineri M, Macchi A, et al. 2013 Custom-made, selective laser sintering (SLS) blade implants as a non-conventional solution for the prosthetic rehabilitation of extremely atrophied posterior mandible *Lasers in Medical Science*. **28** 1241-7
9. Schantz JT, Hutmacher DW, Lam CFX, Brinkmann M, Wong KM, Lim TC, et al. 2003 Repair of calvarial defects with customised tissue-engineered bone grafts - II. Evaluation of cellular efficiency and efficacy *in vivo* *Tissue Eng*. **9** S127-S39
10. Warnke PH, Springer ING, Wiltfang J, Acil Y, Eufinger H, Wehmoller M, et al. 2004 Growth and transplantation of a custom vascularised bone graft in a man *Lancet*. **364** 766-70
11. Warnke PH, Wiltfang J, Springer I, Acil Y, Bolte H, Kosmahl M, et al. 2006 Man as living bioreactor: Fate of an exogenously prepared customized tissue-engineered mandible *Biomaterials*. **27** 3163-7

12. Dyson JA, Genever PG, Dalgarno KW, Wood DJ 2007 Development of custom-built bone scaffolds using mesenchymal stem cells and apatite-wollastonite glass-ceramics *Tissue Eng.* **13** 2891-901
13. Xiao K, Dalgarno KW, Wood DJ, Goodridge RD, Ohtsuki C 2008 Indirect selective laser sintering of apatite-wollastonite glass-ceramic *Proceedings of the Institution of Mechanical Engineers Part H-Journal of Engineering in Medicine.* **222** 1107-14
14. Kokubo T 1991 Bioactive glass-ceramics - properties and applications *Biomaterials.* **12** 155-63
15. Kokubo T, Ito S, Shigematsu M, Sakka S, Yamamuro T 1985 Mechanical-properties of a new type of apatite-containing glass ceramic for prosthetic application *Journal of Materials Science.* **20** 2001-4
16. Ohsawa K, Neo M, Okamoto T, Tamura J, Nakamura T 2004 In vivo absorption of porous apatite- and wollastonite-containing glass-ceramic *Journal of Materials Science-Materials in Medicine.* **15** 859-64
17. Kokubo T. Bioceramics and their clinical applications. In: Yamamuro T, editor. Clinical application of bioactive glass-ceramics. 9 ed: Woodhead Publishing; 2008. p. 583-605.
18. Damien E, Hing K, Saeed S, Revell PA 2003 A preliminary study on the enhancement of the osteointegration of a novel synthetic hydroxyapatite scaffold in vivo *Journal of Biomedical Materials Research Part A.* **66A** 241-6
19. Zhang H, Ye XJ, Li JS 2009 Preparation and biocompatibility evaluation of apatite/wollastonite-derived porous bioactive glass ceramic scaffolds *Biomaterials.* **4**
20. Meirelles LDS, Chagastelles PC, Nardi NB 2006 Mesenchymal stem cells reside in virtually all post-natal organs and tissues *Journal of Cell Science.* **119** 2204-13
21. Pittenger MF, Mackay AM, Beck SC, Jaiswal RK, Douglas R, Mosca JD, et al. 1999 Multilineage potential of adult human mesenchymal stem cells *Science.* **284** 143-7
22. Bruder SP, Kraus KH, Goldberg VM, Kadiyala S 1998 The effect of implants loaded with autologous mesenchymal stem cells on the healing of canine segmental bone defects *Journal of Bone and Joint Surgery-American Volume.* **80A** 985-96
23. C H. Selective laser sintering of stainless steel powder. Leeds: University of Leeds: School of Mechanical Engineering; 2003.
24. Xiao C. Indirect SLS of Apatite-Wollastonite Glass-Ceramic. Leeds: University of Leeds: School of Mechanical Engineering; 2007.

25. Etheridge SL, Spencer GJ, Heath DJ, Genever PG 2004 Expression profiling and functional analysis of Wnt signaling mechanisms in mesenchymal stem cells *Stem Cells*. **22** 849-60
26. de Vries A, Paton JFR, Lightman SL, Lowry CA 2005 Characterisation of c-Fos expression in the central nervous system of mice following right atrial injections of the 5-HT3 receptor agonist phenylbiguanide *Autonomic Neuroscience-Basic & Clinical*. **123** 62-75
27. Vickers W. The Effect of Strontium Substitution on Apatite-Wollastonite Glass-Ceramics. University of Leeds; 2013.
28. Kokubo T, Ito S, Sakka S, Yamamuro T 1986 Formation of high-strength bioactive glass cermaic in the system MgO-CaO-SiO<sub>2</sub>-P<sub>2</sub>O<sub>5</sub> *Journal of Materials Science*. **21** 536-40
29. Mygind T, Stiehler M, Baatrup A, Li H, Zoua X, Flyvbjerg A, et al. 2007 Mesenchymal stem cell ingrowth and differentiation on coralline hydroxyapatite scaffolds *Biomaterials*. **28** 1036-47
30. Stiehler M, Bunger C, Baatrup A, Lind M, Kassem M, Mygind T 2009 Effect of dynamic 3-D culture on proliferation, distribution, and osteogenic differentiation of human mesenchymal stem cells *J Biomed Mater Res Part A*. **89A** 96-107
31. Sikavitsas VI, Bancroft GN, Mikos AG 2002 Formation of three-dimensional cell/polymer constructs for bone tissue engineering in a spinner flask and a rotating wall vessel bioreactor *Journal of Biomedical Materials Research*. **62** 136-48
32. Frith JE, Thomson B, Genever PG 2010 Dynamic Three-Dimensional Culture Methods Enhance Mesenchymal Stem Cell Properties and Increase Therapeutic Potential *Tissue Engineering Part C-Methods*. **16** 735-49
33. Fujita H, Iida H, Ido K, Matsuda Y, Oka M, Nakamura T 2000 Porous apatite-wollastonite glass-ceramic as an intramedullary plug *Journal of Bone and Joint Surgery-British Volume*. **82B** 614-8
34. Holtorf HL, Jansen JA, Mikos AG 2005 Ectopic bone formation in rat marrow stromal cell/titanium fiber mesh scaffold constructs: Effect of initial cell phenotype *Biomaterials*. **26** 6208-16
35. van den Dolder J, Vehof JWM, Spauwen PHM, Jansen JA 2002 Bone formation by rat bone marrow cells cultured on titanium fiber mesh: Effect of in vitro culture time *Journal of Biomedical Materials Research*. **62** 350-8
36. Castano-Izquierdo H, Alvarez-Barreto J, van den Dolder J, Jansen JA, Mikos AG, Sikavitsas VI 2007 Pre-culture period of mesenchymal stem cells in osteogenic media influences their in vivo bone forming potential *J Biomed Mater Res Part A*. **82A** 129-38

## Figure Legends

**Figure 1.** Structure of bA-W and cA-W scaffolds. bA-W scaffolds were designed with dimensions of 3x3x2mm (A) and cA-W scaffolds with dimensions of 5x5x2mm containing a central channel (arrows) 1mm in diameter (B). Both of which were produced by SLS. A2 and B2 show SEM images to demonstrate the surface structure and porosity of the bA-W and cA-W scaffolds respectively. C1 shows surface topography of A-W, whilst C2 shows a typical fracture surface of an A-W scaffold, demonstrating the internal structure and porosity. Scale bars; A2 and B2 = 1000µm, C1 and C2 = 200µm.

**Figure 2.** XRD pattern for cA-W after heat treatment showing apatite (■) and wollastonite (◆) phases, referenced from ICDD15-876/42-547.

**Figure 3.** Optimisation of seeding density on cA-W and bA-W scaffolds for dynamic culture. cA-W scaffolds were seeded with  $1 \times 10^6$  (A),  $1.5 \times 10^6$  (B) or  $2 \times 10^6$  (C) MSCs per scaffold and bA-W scaffolds were seeded with  $5 \times 10^5$  (D) or  $1 \times 10^6$  (E) MSCs per scaffold. The scaffolds were analysed by SEM after 24 hours dynamic culture in basal medium. Arrows identify sheets of cells and \* indicates bare A-W scaffold. Scale bars = 500µm (left column) and 200µm (right column), representative images shown, n=3.

**Figure 4.** Cell viability of MSCs dynamically cultured on cA-W scaffolds. MSCs were dynamically cultured under osteogenic conditions and their viability was determined using a fluorescent live/dead assay under confocal microscopy at 0, 7, 14 and 21 days after induction. The majority of MSCs retained viability (left panel; green fluorescence identifies viable cells) for up to 21 days although there appeared a few dead cells (the right panel; red fluorescence identifies the nuclei of dead cells). Day 0 depicted here is equivalent to Day 1 basal medium. Scale bar = 200µm, representative images shown, n=3.

**Figure 5.** Time course SEM analysis of cell growth on cA-W scaffolds. Scaffolds were seeded with  $2 \times 10^6$  MSCs per scaffold and analysed by SEM after 0, 7, 14 and 21 days of dynamic culture in osteogenic medium. The MSCs formed a confluent monolayer of cells on all surfaces of the scaffolds and by day 14 the central channel (arrows) was covered by cells/matrix, representative images shown,  $n=3$ .

**Figure 6.** Sanderson's rapid bone stain after 4 weeks subcutaneous implantation. bA-W (*A, B*) and cA-W (*C, D*) scaffolds were seeded with MSCs, cultured for 7 days in osteogenic medium (*A* and *C*) or 1 day in basal medium (*B* and *D*) and implanted subcutaneously in nude mice for 4 weeks. Control un-seeded cA-W (*E*). Positive blue/green staining, particularly in the pores and around the periphery of the cell-seeded scaffolds (\*), indicates osteoid and soft tissue formation. *A1-E1* and *A2-E2* shows the interface between the scaffold and newly formed tissue at different magnifications. *C3-E3* shows the central channel of the cA-W scaffolds. Scale bar = 250 $\mu$ m, representative images shown,  $n=4$ .

**Figure 7.** Sanderson's rapid bone stain after 8 weeks subcutaneous implantation. bA-W (*A, B*) and cA-W (*C, D*) scaffolds were seeded with MSCs, cultured for 7 days in osteogenic medium (*A* and *C*) or 1 day in basal medium (*B* and *D*) and implanted subcutaneously in nude mice for 8 weeks. Control un-seeded cA-W (*E*). There was a high level of positive blue/green staining (\*) for osteoid and soft tissue formation. *A1-E1* and *A2-E2* shows the interface between the scaffold and newly formed tissue at different magnifications. *C3-E3* shows the central channel of the cA-W scaffolds. Scale bar = 250 $\mu$ m, representative images shown,  $n=4$ .

**Figure 8.** Alcian blue/sirius red staining after 4 weeks subcutaneous implantation. bA-W (*A, B*) and cA-W (*C, D*) scaffolds were seeded with MSCs, cultured for 7 days in osteogenic medium (*A* and *C*) or 1 day in basal medium (*B* and *D*) and implanted subcutaneously in nude mice for 4 weeks. Control un-seeded cA-W scaffolds (*E*). Positive sirius red staining for collagen was observed. *A1-E1* shows the interface between the scaffold and newly formed tissue, *A2-E2* shows matrix deposition within the scaffolds and *C3-E3* shows the central channel of the cA-W scaffolds. Scale bar = 250 $\mu$ m, representative images shown,  $n=4$ .

**Figure 9.** Macroscopic examination of implanted scaffolds. There was no sign of inflammation around the scaffolds after 4 weeks subcutaneous implantation in nude mice. The scaffolds were well integrated with the host tissue. (A) cA-W scaffold, 1 day basal medium. (B) cA-W scaffold, un-seeded control. Arrows indicate where blood vessel association with the c-A-W scaffolds can be observed, particularly within the central channel, representative images shown, n=4.

Accepted Article

Accepted Article

**Table 1.** Reagents used to make A-W glass.

	<b>MgO</b>	<b>CaCO<sub>3</sub></b>	<b>SiO<sub>2</sub></b>	<b>P<sub>2</sub>O<sub>5</sub></b>	<b>CaF<sub>2</sub></b>
<b>Mass (g)</b>	18.4	319.2	136.0	64.8	2.0

**Table 2.** Scaffold groups for subcutaneous implantation *in vivo* (n = 4).

Group	Scaffold	Seeded with MSCs	Culture medium	<i>In vitro</i> culture time (days)	Implantation time (weeks)
A	bA-W	+	Osteogenic	7	8
B	cA-W	+	Osteogenic	7	8
C	bA-W	+	Basal	1	8
D	cA-W	+	Basal	1	8
E	cA-W	-	Basal	1	8
F	bA-W	+	Osteogenic	7	4
G	cA-W	+	Osteogenic	7	4
H	bA-W	+	Basal	1	4
I	cA-W	+	Basal	1	4
J	cA-W	-	Basal	1	4

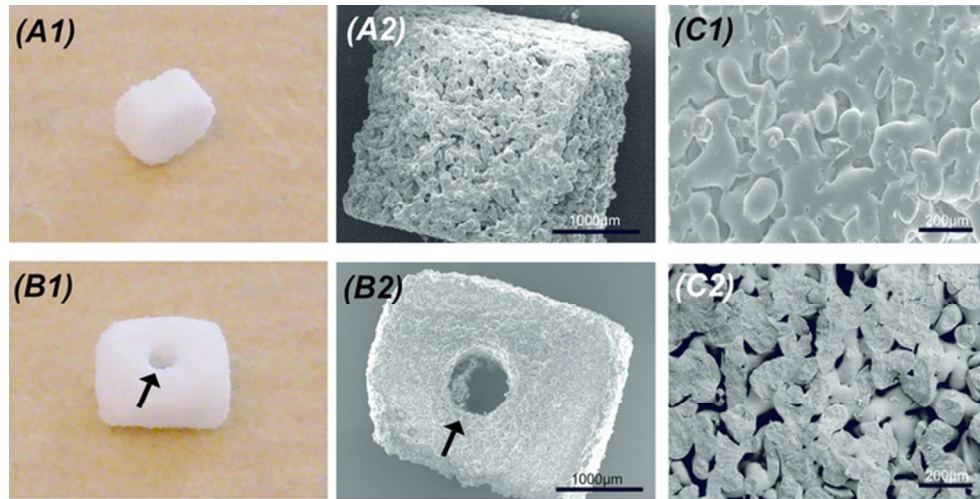


Figure 1  
62x30mm (300 x 300 DPI)

Accepted

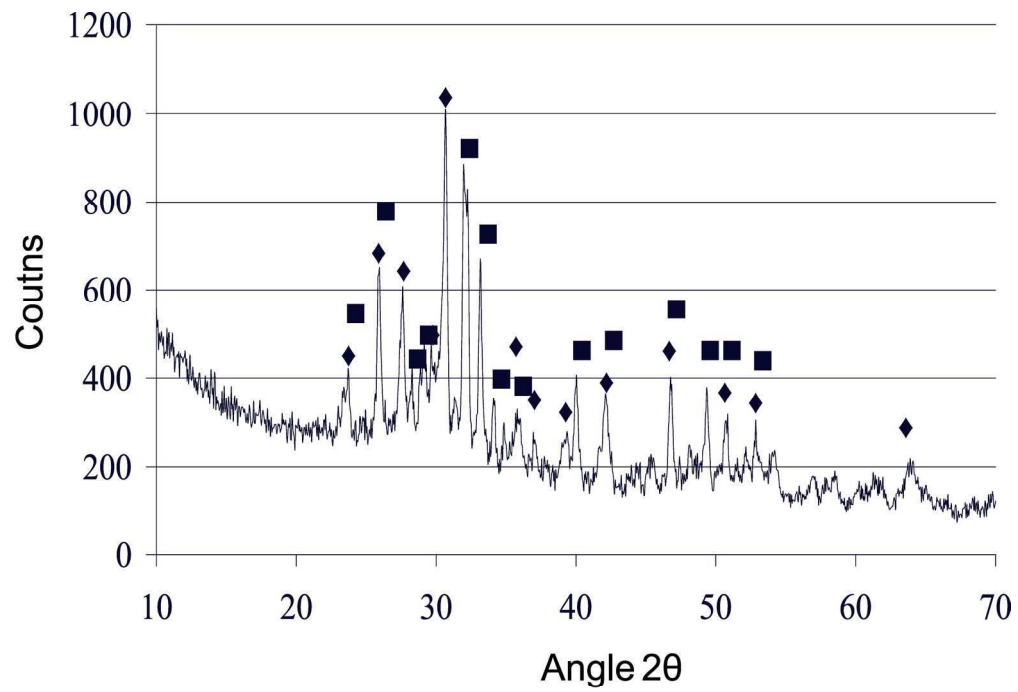


Figure 2  
88x67mm (600 x 600 DPI)

Accept

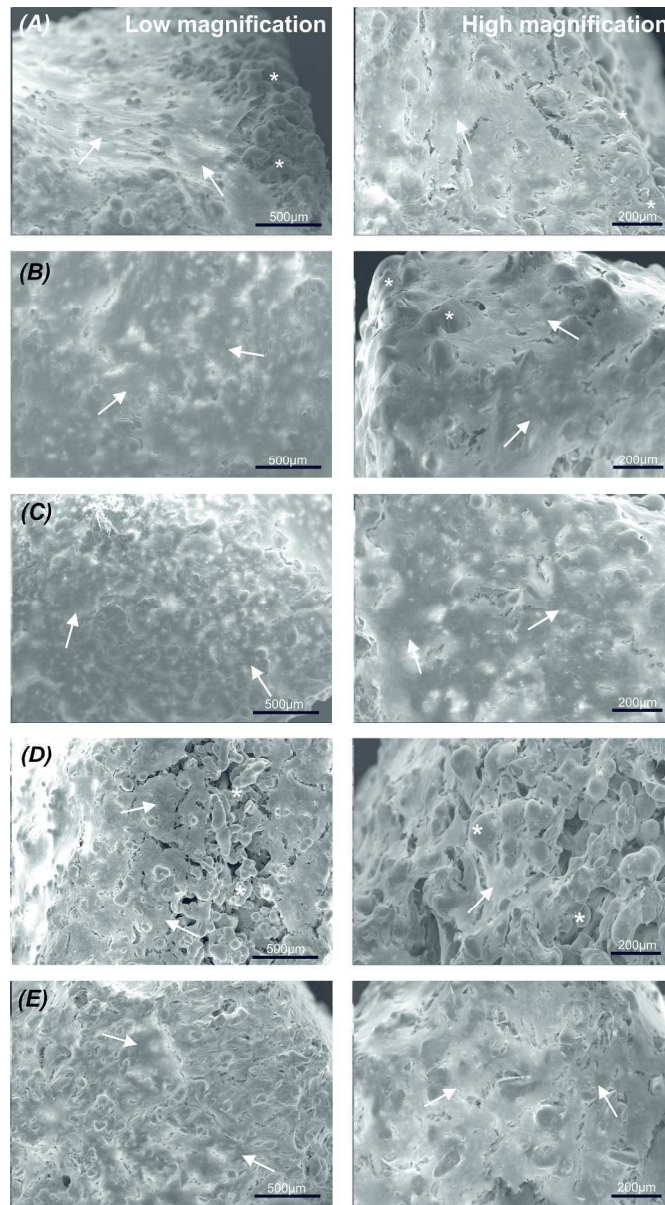


Figure 3  
202x361mm (300 x 300 DPI)

AC

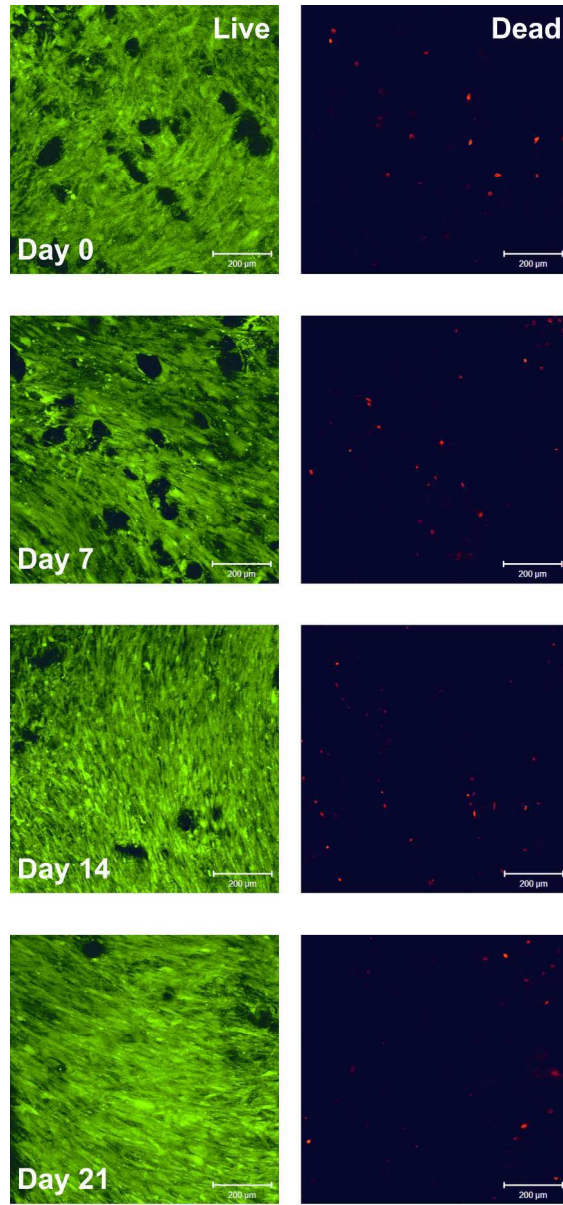


Figure 4  
161x342mm (300 x 300 DPI)

AC

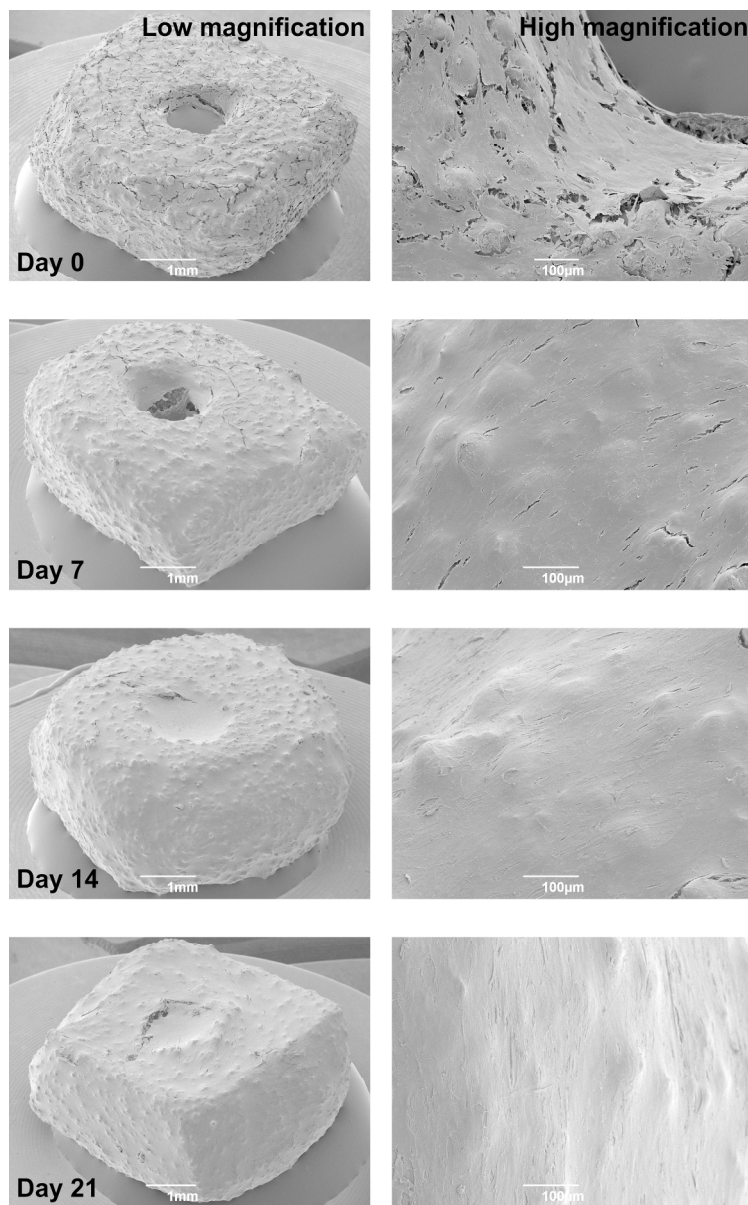


Figure 5  
182x290mm (300 x 300 DPI)

AC

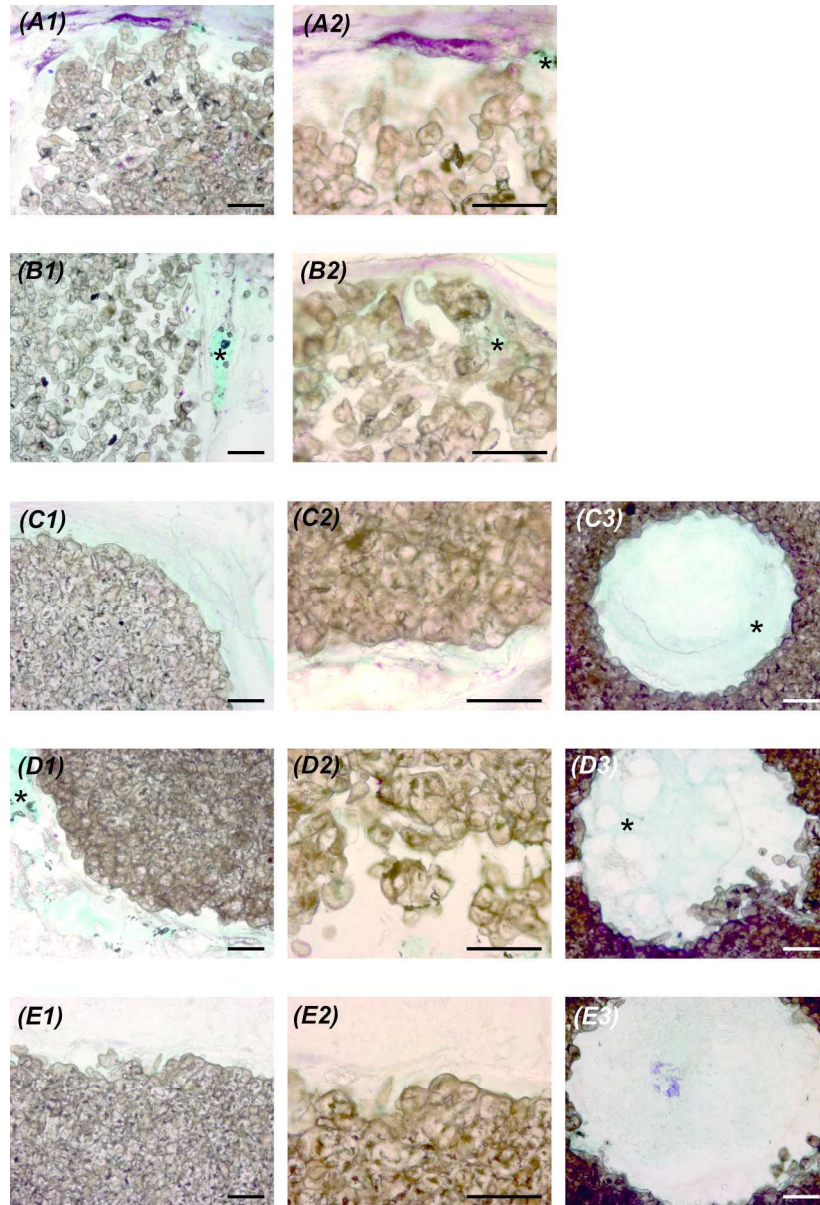


Figure 6  
190x279mm (300 x 300 DPI)

AC

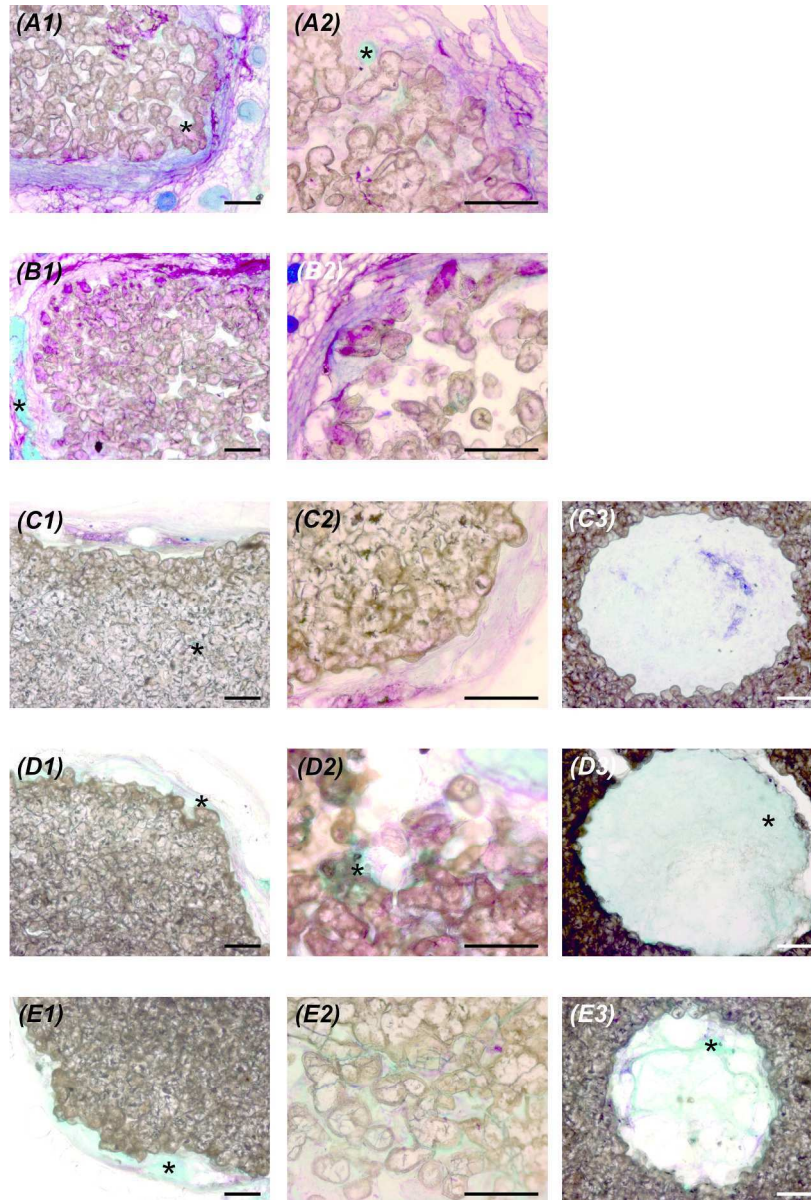


Figure 7  
192x283mm (300 x 300 DPI)

AC

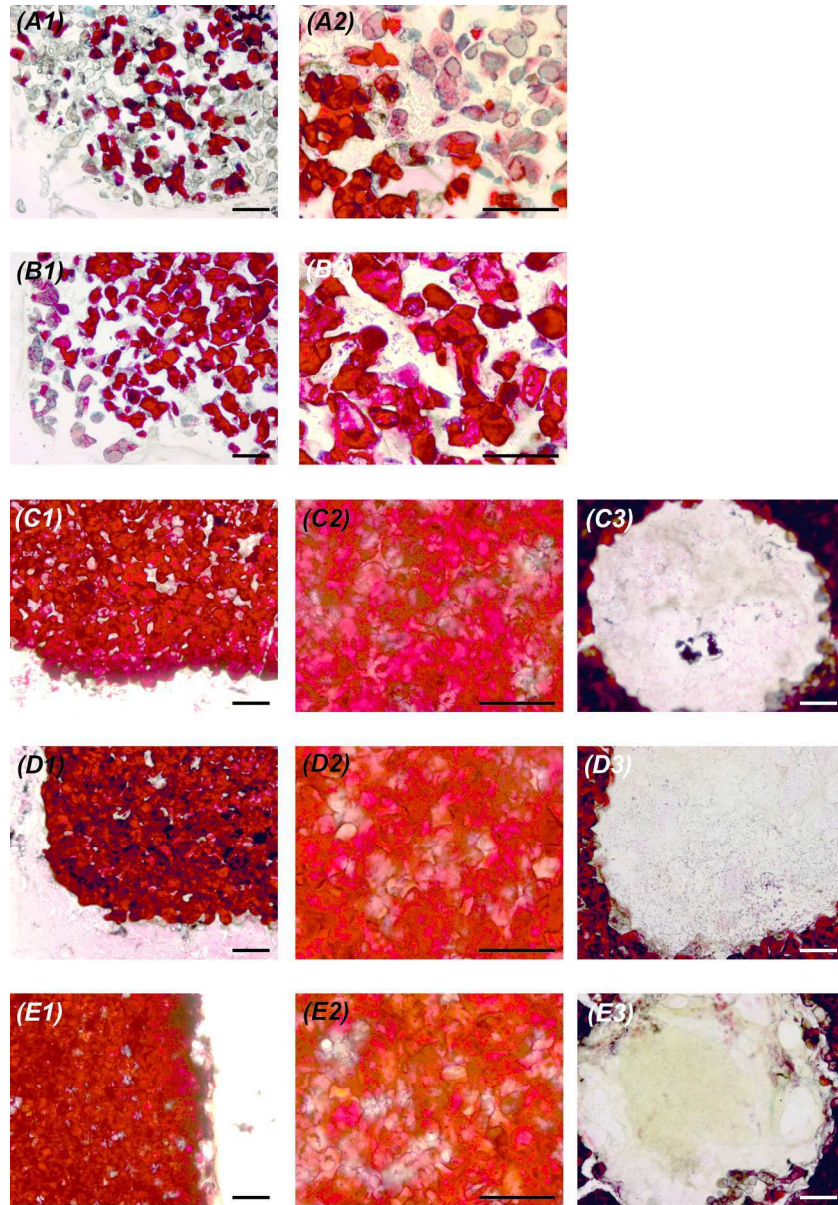


Figure 8  
187x269mm (300 x 300 DPI)

AC

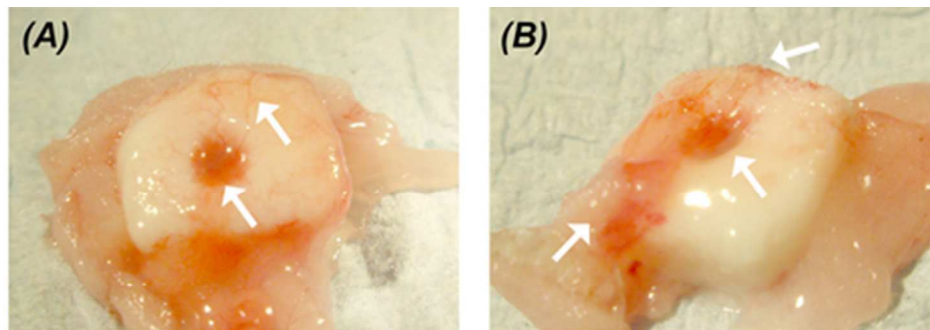


Figure 9  
41x15mm (300 x 300 DPI)

Accepted A